Geometric optics interpretation for rainbow scattering of a chiral sphere

Zhensen Wu (吴振森)[1,2,*], Qingchao Shang (尚庆超)[1], Tan Qu (屈 檀)[1], Zhengjun Li (李正军)[1], and Lu Bai (白 璐)[1]

[1]*School of Physics and Optoelectronic Engineering, Xidian University, Xi'an 710071, China*
[2]*Collaborative Innovation Center of Information Sensing and Understanding at Xidian University, Xi'an 710071, China*
**Corresponding author: wuzhs@mail.xidian.edu.cn*

Received September 11, 2015; accepted October 27, 2015; posted online December 7, 2015

Research on light scattering from a large chiral sphere shows that the rainbow phenomenon is different from that of an isotropic sphere. A chiral sphere with certain chirality generates three first-order rainbows. In this Letter, we present a geometric optics interpretation for the phenomenon and make a calculation of the rainbow angles. The ray traces inside the sphere are determined by the reflection and refraction laws of light at the achiral–chiral interface and the chiral–achiral interface. The calculated rainbow angles achieve good agreements with those obtained by the analytical solutions. The effects of chirality and the refractive index of the sphere on rainbow angles are analyzed.

OCIS codes: 160.1585, 080.0080, 290.5850.
doi: 10.3788/COL201513.121602.

The rainbow phenomenon of an isotropic sphere can be described properly by using both Lorenz–Mie theory and geometric optics[1–4]. Related research has been applied in measurements of particle characteristics such as size and velocity[5]. Chiral media, also known as the "optical active media" at optical frequencies, have been researched a lot in the past several decades due to their different optical and electromagnetic properties[6]. Research on light scattering from large-sized chiral spheres[7,8] has shown that for a linearly polarized wave incidence, there are three first-order rainbow structures. The phenomenon is numerically analyzed based on analytical solutions[9].

In this Letter, we present a geometric optics model to compute the rainbow angles of a chiral sphere based on the optical properties of chiral media. A light wave propagates in chiral media in circularly polarized modes, which is different from the way light travels in general isotropic media. For a chiral medium, there are two different wave numbers for different handednesses of polarized light at one frequency. According to the electromagnetic description of a chiral medium, the wave numbers of a right-handed circularly polarized (RCP) wave and a left-handed circularly polarized (LCP) wave in a chiral medium are $k_R = k_0(n_c + \kappa)$ and $k_L = k_0(n_c - \kappa)$, respectively. k_0 is the wave number of the light wave in vacuum, κ is the chirality parameter of the medium, and n_c is a parameter related to the permittivity and the permeability of the medium. Thus, it can be considered that there is a refractive index for an RCP wave, which is $n_R = n_c + \kappa$; for an LCP wave, it is $n_L = n_c - \kappa$. In the figures, the RCP rays are denoted by the red lines, and the LCP rays are denoted by the blue lines. For convenience, all media considered in this Letter are lossless media.

Before we research the ray traces in a chiral sphere, an introduction to the reflection and refraction of light at the achiral–chiral interface and the chiral–achiral interface is necessary. Much study was devoted to it several years ago[10–13]. Consider a light ray impinging on an achiral–chiral interface with an incidence angle θ_i, as shown in Fig. 1(a). n_0 is the refractive index of the isotropic medium and k_i is the wave number of the incident light. There will be two transmitted rays in the chiral medium. One is an RCP ray with refracted angle θ_R and the other is an LCP ray with refracted angle θ_L. The continuity of the tangential components of the wave vectors in the two regions leads to

$$n_0 \sin\theta_i = n_R \sin\theta_R = n_L \sin\theta_L, \tag{1}$$

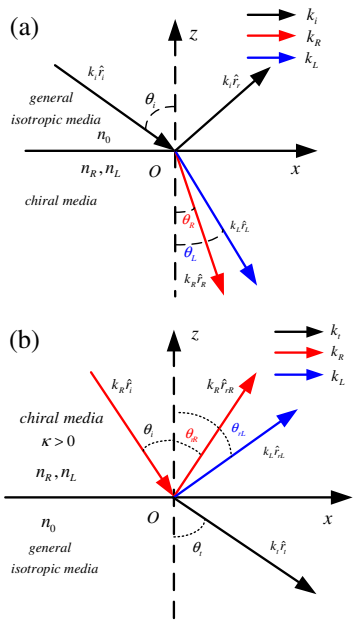

Fig. 1. Light interaction with chiral interface. (a) Achiral–chiral interface. (b) Chiral–achiral interface.

from which follow the two refracted angles:

$$\sin\theta_R = n_0/n_R \sin\theta_i, \qquad \sin\theta_L = n_0/n_L \sin\theta_i. \quad (2)$$

At the chiral–achiral interface, suppose that an RCP ray illuminates the interface with an incident angle θ_i. There will be two reflected rays in the chiral medium and one transmitted ray in the general isotropic medium, as shown in Fig. 1(b). Similarly, the reflected angles and the refracted angle can be obtained by:

$$n_R \sin\theta_i = n_R \sin\theta_{rR} = n_L \sin\theta_{rL} = n_0 \sin\theta_t. \quad (3)$$

It can be seen that, the reflected angle of the reflected RCP ray is equal to the incident angle $\theta_{rR} = \theta_i$, while the reflected angle of the reflected LCP ray is obtained by $\sin\theta_{rL} = n_R/n_L \sin\theta_i$ and the refracted angle of the transmitted ray is obtained by $\sin\theta_t = n_R/n_0 \sin\theta_i$. In the same way, if the incident light is LCP, there will be a reflected RCP ray and a reflected LCP ray, and the reflected angle of the reflected LCP ray will equal the incident angle. The reflected angle of reflected RCP ray can be obtained by $\sin\theta_{rR} = n_L/n_R \sin\theta_{rL}$.

According to the geometric optics model for rainbows of isotropic spheres[3], the first-order rainbow is formed by transmitted rays after one internal reflection of the incident light ray. Similarly, to explain first-order chiral sphere rainbows and calculate the rainbow angles, we need to determine the transmitted rays after one internal reflection. According to the illustration of the light interaction with the chiral interface in Fig. 1, it can be inferred that a linearly polarized ray incident at the surface of a chiral sphere generates a refracted RCP ray and a refracted LCP ray inside the sphere. Each refracted ray inside the sphere generates two reflected rays after one internal reflection. Thus, there are four total transmitted rays outside the sphere after one internal reflection.

A sketched map of the light rays interacting with a chiral sphere is illustrated in Fig. 2. The two refractive indices of the chiral sphere are n_R and n_L. The refractive index of the surrounding medium is n_1. In the figure, A, B, C, D, E, F, and G denote points of intersections of rays and the sphere's surface. O denotes the center of the sphere. Figure 2(a) illustrates ray AC (the refracted RCP ray) and its following traces. Figure 2(b) illustrates ray AB (the refracted LCP ray) and its following traces. In Fig. 2(a), AC generates a reflected RCP ray and a reflected LCP ray, respectively denoted by CG and CE. Then, CG generates transmitted ray RR outside the sphere, and CE generates transmitted ray RL. In Fig. 2(b), AB generates reflected RCP ray BF and reflected LCP ray BD, producing transmitted rays LR and LL, respectively.

By applying the reflection and refraction laws of light at the chiral interface presented above, ray traces in the chiral sphere can be determined. In Fig. 2, the incident angle is denoted by θ_i; the refracted angle of the refracted RCP ray, i.e., $\angle OAC$, is denoted by θ_R, and the refracted angle of the refracted LCP ray, i.e., $\angle OAB$, is denoted by θ_L.

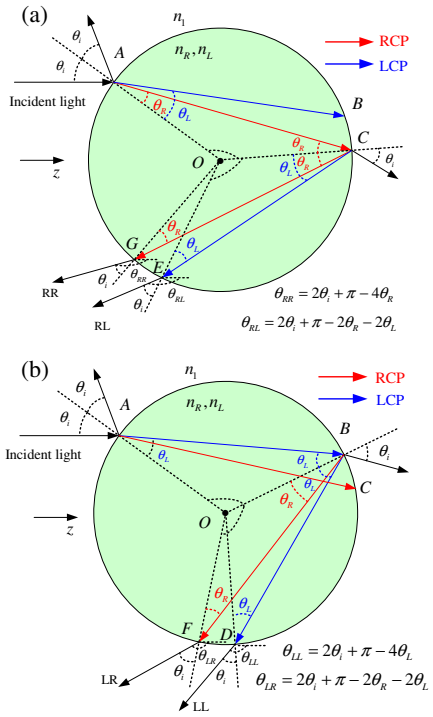

Fig. 2. Light interaction with the chiral sphere. (a) AC and its following traces. (b) AB and its following traces.

According to Eq. (1), the three angles satisfy the following relations: $n_1 \sin\theta_i = n_R \sin\theta_R = n_L \sin\theta_L$. Inside the sphere, $\angle OCA = \angle OAC = \theta_R$. Thus, considering the internal reflection at point C, the incident angle is θ_R. According to Eq. (3), the two reflected angles follow: $\angle OCG = \theta_R$, $\angle OCE = \theta_L$. Then at point G and point E, the incident angles are θ_R and θ_L, respectively. Subsequently, the corresponding refracted angles are found to be both equal to θ_i. Thus, rays RR and RL can be determined. Rays AB, BF, BD, LR, and RL in Fig. 2(b) can be determined similarly.

With the above angles determined, the directions of the final transmitted rays can be computed. The transmitted directions are specified by the deviation angles of the transmitted rays from the positive z-axis, denoted by θ_{RR}, θ_{RL}, θ_{LR}, and θ_{LL}. According to the illustrations in the figure, these angles can be readily derived using the following:

$$\theta_{RR} = 2\theta_i + \pi - 4\theta_R, \quad (4)$$

$$\theta_{RL} = 2\theta_i + \pi - 2\theta_R - 2\theta_L, \quad (5)$$

$$\theta_{LR} = 2\theta_i + \pi - 2\theta_R - 2\theta_L, \quad (6)$$

$$\theta_{LL} = 2\theta_i + \pi - 4\theta_L, \quad (7)$$

where $\theta_R = \arcsin(n_1/n_R \sin\theta_i)$ and $\theta_L = \arcsin(n_1/n_L \sin\theta_i)$.

By comparing ray traces in Figs. 2(a) and 2(b), we have $\angle AOC = \angle BOF$, $\angle COE = \angle AOB$, thus obtaining

$$\angle AOC + \angle COE = \angle AOB + \angle BOF, \tag{8}$$

which implies that point E and point F are superposed. From Eqs. (5) and (6), it can be seen that $\theta_{RL} = \theta_{LR}$; therefore, RL and LR are also superposed. This means that the number of final transmitted rays after one internal reflection is three, instead of four. The traces of a linearly polarized incident ray impinging on a chiral sphere are depicted in Fig. 3.

Taking a further step past Eqs. (4)–(7), the transmitted directions of the three transmitted rays are derived as functions of the incident angle:

$$\theta_{RR} = 2\theta_i + \pi - 4\ \arcsin(n_1/n_R\ \sin\ \theta_i), \tag{9}$$

$$\theta_{LL} = 2\theta_i + \pi - 4\ \arcsin(n_1/n_L\ \sin\ \theta_i), \tag{10}$$

$$\theta_{RL/LR} = 2\theta_i + \pi - 2\ \arcsin(n_1/n_R\ \sin\ \theta_i) - 2\ \arcsin(n_1/n_L\ \sin\ \theta_i). \tag{11}$$

As the incident angle varies from 0 to $\pi/2$, the three deviation angles, θ_{RR}, θ_{LL}, and θ_{RL}, pass through their own extrema, which form the first-order rainbows. For θ_{RR} and θ_{LL}, the extrema can be readily determined by the following expressions:

$$\theta^{\text{ext}}_{RR,LL} = 2\theta_i^{RR,LL} + \pi - 4\ \arcsin(n_1/n_{R,L}\ \sin\ \theta_i^{RR,LL}), \tag{12}$$

$$\theta_i^{RR} = \arcsin\sqrt{\frac{4}{3} - \frac{1}{3(n_1/n_R)^2}}, \tag{13}$$

$$\theta_i^{LL} = \arcsin\sqrt{\frac{4}{3} - \frac{1}{3(n_1/n_L)^2}}, \tag{14}$$

where θ^{ext}_{RL}, the extremum of θ_{RL}, can be computed by numerical methods.

The extrema of the three deviation angles, θ^{ext}_{RR}, θ^{ext}_{LL}, and θ^{ext}_{RL}, construct the three rainbow angles of a chiral sphere. From Eqs. (9)–(11), it can be seen that formulations of the rainbow angles for RR and LL are the same as that of a general isotropic sphere. Both AC and CG are RCP rays. For traces including incident light, AC, CG, and RR, the chiral sphere can be regarded as an isotropic sphere with refractive index n_R. For traces including incident light, AB, BD, and LL, the chiral sphere can be regarded as an isotropic sphere with refractive index n_L. It seems that θ^{ext}_{RR} and θ^{ext}_{LL} are just the rainbow angles of an isotropic sphere with refractive index n_R and n_L, respectively. However, the rainbow angle θ^{ext}_{RL} is determined by both n_R and n_L. Besides, note that according to Eq. (14), $n_{R,L} < 2n_1$ is a necessary condition for the rainbow phenomenon of a chiral sphere.

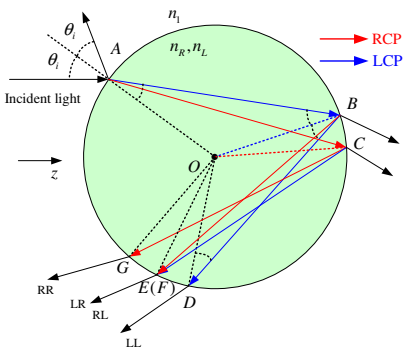

Fig. 3. Final ray traces in the chiral sphere.

In order to examine the model, we calculate the rainbow angles by using the above expressions and compare them with the rainbow structure calculated by analytical solutions. Figure 4 presents the rainbow structures of a chiral sphere in Ref. [8], along with the rainbow angles calculated by the geometric model in this Letter. The three rainbows are named the "right rainbow," "middle rainbow," and "left rainbow," according to their relative positions. The radius of the sphere is 500 times the light wavelength, and $n_c = 1.33$. The chirality parameter is $\kappa = 0.08$, and surrounding medium is the vacuum. Thus, we have $n_R = 1.41$, $n_L = 1.25$, and $n_1 = 1.0$. The rainbow angles, i.e., the extrema of θ_{RR}, θ_{RL}, and θ_{LL} based on Eqs. (9)–(11), are computed as: $\theta^{\text{ext}}_{RR} = 147.93°$, $\theta^{\text{ext}}_{RL} = 136.50°$, and $\theta^{\text{ext}}_{LL} = 124.10°$. As we know, there is little difference between the peak angle of the rainbow structure and the rainbow angle. It can be seen that the three rainbow angles computed by the geometric model agrees well with the analytical solutions. As light propagates inside the chiral sphere in circularly polarized modes, rainbows occur in both the E-plane ($\phi = 0°$) and the H-plane ($\phi = 90°$), which are different from those of an isotropic sphere. We also calculate the rainbow angle of an isotropic sphere ($\kappa = 0.0$), which denoted by θ_{Iso} in Fig. 4(b). $\theta_{\text{Iso}} = 137.48°$ shows that the

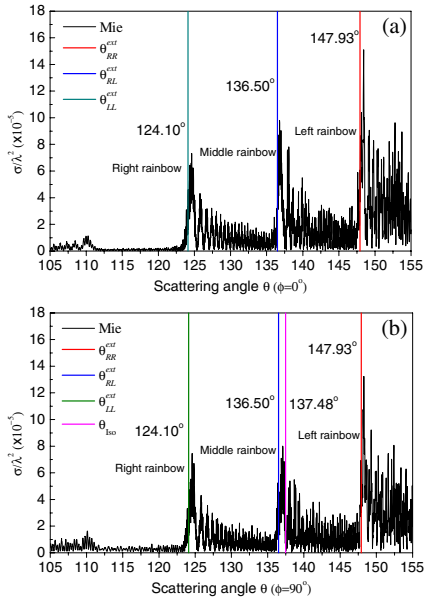

Fig. 4. Rainbow angles compared with analytical solutions. $a = 500\lambda$, $\varepsilon_r = 1.7689$, $\mu_r = 1.0$ (i.e., $n_c = 1.33$), and $\kappa = 0.08$. (a) E-plane. (b) H-plane.

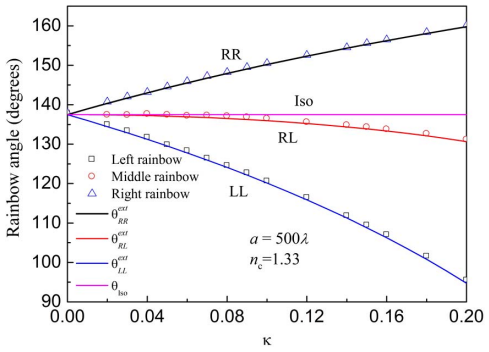

Fig. 5. Variation of rainbow angles with chirality.

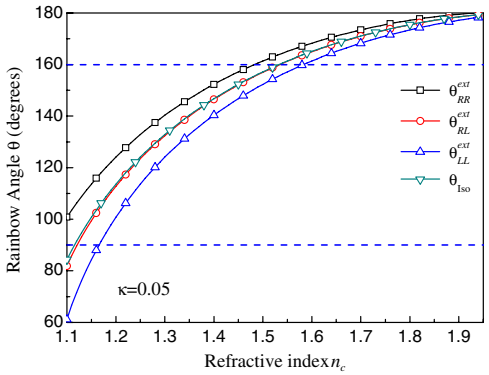

Fig. 6. Effects of refractive index of the chiral sphere.

rainbow angle of the isotropic sphere is not equal to that of the middle rainbow of the chiral sphere.

It is convenient to use the geometric model to analyze the variation of the rainbow angles. They can be computed by formulas directly. Figure 5 presents the variation of the three rainbow angles of a chiral sphere with the chirality parameter calculated by the geometric model, compared with the peak angles of the rainbow structures presented in Ref. [9]. It can be seen that the rainbow angles calculated by the geometric model in this Letter achieve good agreement with those from the analytical work. Note that the rainbow angle of the middle rainbow varies slightly with the chirality. In fact, the result is readily understandable if we note that the two refractive indices for a chiral medium are $n_R = n_c + \kappa$ for the RCP wave and $n_L = n_c - \kappa$ for the LCP wave. For a larger chirality parameter, the difference between n_R and n_L is larger. It seems that the left rainbow angle, $\theta_{LL}^{\mathrm{ext}}$, is more sensitive to the variation of the chirality parameter than the other two.

Figure 6 shows the variation of the rainbow angles with the parameter n_c of the chiral sphere. The chirality parameter is $\kappa = 0.05$; therefore, $n_{R,L} = n_c \pm 0.05$. n_c varies from 1.1 to 1.94 with a step of 0.01. It can be seen that as n_c increases, all three rainbow angles increase, while the differences between them get smaller. The curves in the figure calculated by the geometric optics model cover large angle range, from 60° to 180°. However, according to the analytical solutions, a rainbow only occurs in a certain angle range, usually 90°–160°. The rainbow intensity gradually decreases and vanishes eventually when their positions move in a forward or backward direction.

In conclusion, we perform a primary analysis of the rainbow angles of a chiral sphere using a geometric optics model. The key point of the model is that a ray incident on the chiral sphere splits into two transmitted rays inside the sphere and a ray inside the sphere generates two reflected rays after the internal reflection. Based on the model, rainbow angles can be computed directly from formulas, instead of finding peak angles from the angular distributions of the scattering intensity. It is convenient to evaluate the relationship between the rainbow angles and parameters of the sphere. Further work can be done to study the geometric optics model for light scattering from a chiral sphere.

This work was supported by the National Natural Science Foundation of China (Nos. 61172031, 61308025, 61475123, and 61571355) and the Fundamental Research Funds for the Central Universities.

References

1. C. F. Bohren and D. R. Huffman, *Absorption and Scattering of Light by Small Particles* (Wiley, 1998).
2. J. D. Walker, Am. J. Phys. **44**, 421 (1976).
3. H. C. v. d. Hulst, *Light Scattering by Small Particles* (Wiley, 1957).
4. J. A. Adam, Phys. Rep.: Rev. Sect. Phys. Lett. **356**, 229 (2002).
5. J. P. A. J. van Beeck and M. L. Riethmuller, Appl. Opt. **35**, 2259 (1996).
6. A. Lakhtakia, V. K. Varadan, and V. V. Varadan, *Time-Harmonic Electromagnetic Fields in Chiral Media, Lecture Notes in Physics*, Vol. **335** (Springer, 1989).
7. C. F. Bohren, Chem. Phys. Lett. **29**, 458 (1974).
8. Z.-S. Wu, Q.-C. Shang, and Z.-J. Li, Appl. Opt. **51**, 6661 (2012).
9. Q.-C. Shang, Z.-S. Wu, T. Qu, Z.-J. Li, L. Bai, and L. Gong, Opt. Express **21**, 21879 (2013).
10. L. John, Pure Appl. Opt.: J. Eur. Opt. Soc. Part A **5**, 417 (1996).
11. D. L. Jaggard and X. Sun, J. Opt. Soc. Am. A **9**, 804 (1992).
12. S. Bassiri, C. Papas, and N. Engheta, J. Opt. Soc. Am. A. **5**, 1450 (1988).
13. A. I. Miteva and I. J. Lalov, J. Phys.: Condens. Matter **3**, 529 (1991).